Natural hand posture determination using control-oriented inter-finger coordination kinematic models

Nina Robson*

California State University, Fullerton, California, USA Email: nrobson@fullerton.edu *Corresponding author

Jong-Seob Won

Jeonju University, Jeonju, South Korea Email: jswon@jj.ac.kr

Abstract: The paper builds up on a recently developed planar control-oriented finger kinematic model for natural grasping, based on thumb-long finger(s) anthropometric data. In the model, the posture is determined by the time-dependent radius R of a virtual cylinder encompassed by the fingers. After the experimental evaluation of the model, the results are combined with circle configuration techniques based on the Pedoe maps, to explore the relation between the fingertip-object curvature within the contact and the configuration parameter R for precision grasping. Within the proposed contact geometry setup the fingertip and object curvatures are represented by circles with different radii. The type of interaction is described by defining a configuration matrix. Six fingertip grasping configurations are considered, each of which is constructed from five available circles: two for the fingertips, one virtual circle, and two at the fingertip-object contact points. The results from the case study show that it is possible to calculate the configuration control parameter R based on the choice of any four circles. The preliminary results could further benefit the field of postural synergies and object manipulation, and open the door to the definition of novel kinematic tasks and future combined design-control strategies.

Keywords: human motion; Pedoe maps; contact and curvature kinematic constraints.

Reference to this paper should be made as follows: Robson, N. and Won, J-S. (xxxx) 'Natural hand posture determination using control-oriented inter-finger coordination kinematic models', *Int. J. Mechanisms and Robotic Systems*, Vol. x, No. x, pp.xxx–xxx.

Biographical notes: Robson is an Associate Professor and the Director of the Human-Interactive Robotics Lab at the California State University, Fullerton (CSUF). She obtained her PhD in Mechanical Engineering from the University of California, Irvine (UCI) in 2008. His research is in the

2 N. Robson and J-S. Won

broad areas of kinematics, mechanism design, robotics and biomechanics and explores the interplay between mechanism/robot morphology and their interaction with the environment.

Jong-Seob Won received his BS in Mechanical and Precision Engineering from the Pusan National University, Pusan, Korea, in 1988 and MS and PhD in Mechanical Engineering from the Texas A&M University, College Station, in 1998 and 2003, respectively. Currently, he is a Professor with the Department of Mechanical and Automotive Engineering, Jeonju University, Korea. His current research interests include intelligent control of robotic systems.

1 Introduction

The concept of using relative curvature of surfaces in contact to limit the movement of a workpiece was introduced by Rimon and Burdick (1995a, 1995b). They generalised the study of the grasping constraint of a rigid body using the fingers of a mechanical hand by considering the configuration space of movement of the body relative to obstacles formed by the fingers, and introduced the idea of second order mobility of a constrained body. Robson and McCarthy (2007, 2009), Robson and McCarthy (2010) and Robson and Tolety (2011) developed the theoretical framework for the kinematic synthesis of planar and spatial serial mechanical linkages to guide a workpiece that maintains contact with objects or virtual guides in the environment. Robson et al. (2015), Robson and Soh (2018) and Robson and Chen (2019) build up on the developed theoretical framework and proposed techniques on the simultaneous geometric design of planar multi-limb mechanisms for multiple realisable motion tasks in the vicinity of fingertips-object contact. However, the developed methods do not incorporate human-like motion within the mechanisms.

One of the main functions of hand models is to simulate object grasping, realised by the hand coordination. The latter is the combination of finger movements encompassing the inter-joint coordination of each finger and the inter-finger coordination of the hand. The implementation of the multi-finger coordination (Carpinella et al., 2011) can be a pivotal direction of modelling. A variety of research on finger/hand modelling in various points of view has been made in human fingers simulation (Barbagli et al., 2004), finger motion coordination (Kim, 2014; Braido and Zhang, 2004), virtual hand modelling and simulation (Pena-Pitarch et al., 2012; Miyata et al., 2007, 2005; Savescu et al., 2004), articulated human hands (McDonald et al., 2001; Nolker and Ritter, 2002), and so on. Recent work in modelling the process of grasping and active touch by natural and artificial hands considers the implications of a geometrical model accounting for the correlation of degrees of freedom in patterns of more frequent use (postural synergies). Applications of the synergy models to the design and control of artificial hands is illustrated in Bicchi et al. (2011) and Santello et al. (1998). Although this may not hold true for all possible human finger motions, relating such postural synergies in joint space to Cartesian fingers-object contact and curvature constraints has the potential to lead to novel simplified combined design-control strategies for grasping and object manipulation.

This paper is part of our efforts on exploring ways of incorporating natural human motion on conceptual design level, by studying the relation/interaction between fingertips-object within a contact and the control/configuration parameter R, related to grasping posture for precision grasping tasks. This will further enable the development of future combined design-control strategies for naturalistic motion.

2 Background

2.1 Summary of circle configuration theorem

The contents in this section are taken from Kocik (2007) and summarised briefly. Solutions to circle configuration problems are based on Pedoe (1967, 1970, 1957) maps, whose main notion is to map circles in the plane to vectors of a Minkowski space with a pseudo-Euclidean inner product. For example, a circle C of radius r centred at (x, y) is represented by the Pedoe vector $\dot{\pi}(C)$,

$$\dot{\pi}(C) = \begin{bmatrix} b \\ \bar{b} \\ \dot{x} \\ \dot{y} \end{bmatrix} = \begin{bmatrix} 1/r \\ (x^2 + y^2 - r^2)/r \\ x/r \\ y/r \end{bmatrix}$$

where the element b=1/r is a circle curvature, $\bar{b}=(x^2+y^2-r^2)/r$ circle co-curvature and $\dot{x}=x/r,\ \dot{y}=y/r$ reduced positions.

The Pedoe inner product is defined for two circles as follows:

$$<\dot{\pi}(C_1), \ \dot{\pi}(C_1)> = \frac{C_1 * C_2}{2r_1r_2}$$
 (1)

where $C_1 * C_2$ is the Darboux product Darboux (1872) that is defined as the power of a pair of circles: $C_1 * C_2 = d^2 - r_1^2 - r_2^2$ (d = distance between two centres, r_1 , r_2 radius of each circle).

Based on the notion mentioned above, Kocik (2007) found a formula for the radii and positions in the plane for an arbitrary linearly independent circle configuration. To do this, Kocik defined a configuration matrix \mathbf{f} for the set of four circles represented by Pedoe vectors whose element is represented as $f_{ij} = \langle \mathbf{C}_i, \mathbf{C}_j \rangle$, where $\langle \cdot, \cdot \rangle$ is the Pedoe inner product and $\mathbf{C}_i = \dot{\pi}(C_i)$ of a circle C_i . Likewise, a data matrix is defined as the collective representation of the circles: $A = [\mathbf{C}_1 \mid \mathbf{C}_2 \mid \mathbf{C}_3 \mid \mathbf{C}_4]$

The formula describing the relationship of radii and positions among four linearly independent circles arbitrarily located in the plane is

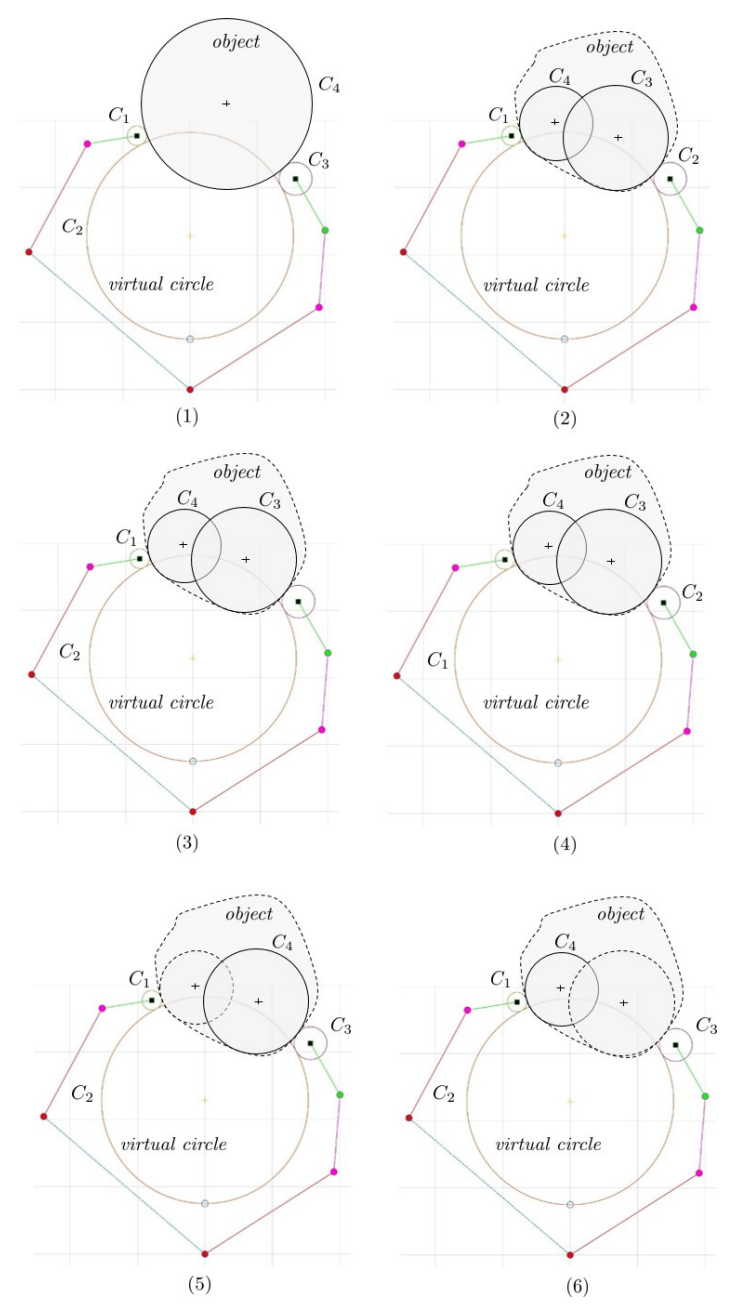
$$\mathbf{AFA}^{\mathrm{T}} = \mathbf{G} \tag{2}$$

where **F** is the inverse matrix of the configuration matrix **f** and $\mathbf{G} = g^{-1}$. g is the matrix of Minkowski metric as:

$$\mathbf{g} = \frac{1}{2} \begin{bmatrix} 0 & 1 & 0 & 0 \\ 1 & 0 & 0 & 0 \\ 0 & 0 & -2 & 0 \\ 0 & 0 & 0 & -2 \end{bmatrix}$$

4 N. Robson and J-S. Won

Figure 1 Circle configuration representation of object-multifinger interaction, fingertip grasping of an object with circular cross-section: (1) TRIO, different configurations for fingertip grasping of an object with different radii of curvatures at the contact: (2) TIO1O2, (3) TRO1O2, (4) RIO1O2, (5) TRIO1 and (6) TRIO2 configuration (see online version for colours)



Notes: The capital letters T, R, I and O represent thumb, virtual circle, index finger and object, respectively.

Equation (2) can be represented by a set of single quadratic formulas for the vector of curvatures and reduced positions, known as Descartes-like formula, generalised to arbitrary independent circle configurations (Descartes, 1901):

$$\mathbf{b}^T F \mathbf{b} = 0 \tag{3}$$

$$\dot{\mathbf{x}}^T F \dot{\mathbf{x}} = -1 \tag{4}$$

$$\dot{\mathbf{y}}^T F \dot{\mathbf{y}} = -1 \tag{5}$$

where

$$\mathbf{b} = \begin{bmatrix} 1/r_1 \\ 1/r_2 \\ 1/r_3 \\ 1/r_4 \end{bmatrix}, \ \dot{\mathbf{x}} = \begin{bmatrix} x_{01}/r_1 \\ x_{02}/r_2 \\ x_{03}/r_3 \\ x_{04}/r_4 \end{bmatrix}, \ \dot{\mathbf{y}} = \begin{bmatrix} y_{01}/r_1 \\ y_{02}/r_2 \\ y_{03}/r_3 \\ y_{04}/r_4 \end{bmatrix}, \ \mathbf{F} = \mathbf{f}^{-1}$$
 (6)

where **b** is a curvature vector, and $\dot{\mathbf{x}}$ and $\dot{\mathbf{y}}$ are reduced position vectors, respectively. **F** is the inverse matrix of a configuration matrix **f**. The first equation is a generalised version of Descartes-like formula for arbitrary independent circle configurations.

The paper combines some of the recently developed naturalistic control-oriented finger kinematic models (Won and Robson, 2019) with circle configuration problems based on the Pedoe map to explore the possibility of determining the posture (most probable joint angle trajectories) defined by a planar thumb and index fingers that are contacting a body. For the problem, it is assumed that the anthropometric data and body geometry within the contacts are known.

As summarised above, equation (2) governs the relation of radii and positions of four circles for an arbitrary circle configuration. Depending on the shape of the object and grasping style (strategies, scenarios, etc), the problem is reduced to the question of selecting any four circles. For fingertip grasping, we consider six configurations, each of which are constructed by four radii of curvature: two for the fingertips, one virtual circle, and two at the fingertip-object contact points (see Figure 1). For example, for the first case shown in Figure 1, the object, the virtual circle and the two fingertips curvatures within the contacts are chosen. In the second case, the two fingertips curvatures and the object curvatures within the contacts are chosen. The circle configuration represents the interaction between fingers and an object. The type of interaction can be described by defining a configuration matrix \mathbf{f} . The entries in the configuration matrix \mathbf{f} are the value of Pedoe inner product between two circles, C_i and C_j . The following is the summary of the Pedoe inner product for a circle configuration.

Case 1 Distant circles:

- Darboux product: $C_i * C_j = d_{ij}^2 r_i^2 r_j^2$.
- Pedoe inner product: $h_{ij} = \frac{C_i * C_i}{2r_i r_j} = \frac{d_{ij}^2 r_i^2 r_j^2}{2r_i r_j}$.

Case 2 Intersecting circles:

• Darboux product: $C_i * C_j = 2r_i r_j \cos \varphi_{ij} \ (= d_{ij}^2 - r_i^2 - r_j^2)$, where φ_{ij} is the angle of intersection made by the two circles.

Case 3 Externally tangent circles [the limiting case of (b) when $\varphi = 0$ rad]:

- Darboux product: $C_i * C_j = 2r_i r_j$.
- Pedoe inner product: $h_{ij} = \frac{C_i * C_j}{2r_i r_j} = 1$.

Case 4 Internally tangent circles [the limiting case of (b) when $\varphi = \pi$ rad]:

- Darboux product: $C_i * C_j = -2r_i r_j$.
- Pedoe inner product: $h_{ij} = \frac{C_i * C_j}{2r_i r_j} = -1$.

The representative interaction includes circles tangent to each other, intersected, and positioned independently.

The configuration matrix \mathbf{f} for each of the six cases in Figure 1 are as follows:

$$\mathbf{f_{TRIO}} = \begin{bmatrix} -1 & 1 & h_{13} & 1 \\ 1 & -1 & 1 & h_{24} \\ h_{31} & 1 & -1 & 1 \\ 1 & h_{42} & 1 & -1 \end{bmatrix}, \quad \mathbf{f_{TIOIO2}} = \begin{bmatrix} -1 & h_{12} & h_{13} & 1 \\ h_{12} & -1 & 1 & h_{24} \\ h_{31} & 1 & -1 & h_{34} \\ 1 & h_{42} & h_{43} & -1 \end{bmatrix},$$

$$\mathbf{f_{TROIO2}} = \begin{bmatrix} -1 & 1 & h_{13} & 1 \\ 1 & -1 & h_{23} & h_{24} \\ h_{31} & h_{32} & -1 & h_{34} \\ 1 & h_{42} & h_{43} & -1 \end{bmatrix}, \quad \mathbf{f_{RIOIO2}} = \begin{bmatrix} -1 & 1 & h_{13} & h_{14} \\ 1 & -1 & 1 & h_{24} \\ h_{31} & 1 & -1 & h_{34} \\ h_{41} & h_{42} & h_{43} & -1 \end{bmatrix},$$

$$\mathbf{f_{TRIO1}} = \begin{bmatrix} -1 & 1 & h_{13} & h_{14} \\ 1 & -1 & 1 & h_{24} \\ h_{31} & 1 & -1 & 1 \\ h_{41} & h_{42} & 1 & -1 \end{bmatrix}, \quad \mathbf{f_{TRIO2}} = \begin{bmatrix} -1 & 1 & h_{13} & 1 \\ 1 & -1 & 1 & h_{24} \\ h_{31} & 1 & -1 & h_{34} \\ 1 & h_{42} & h_{43} & -1 \end{bmatrix}. \quad (7)$$

Note that $h_{ij} = h_{ji}$.

2.2 Kinematic joint rotation configuration models

Incorporating proper postures of fingers that resemble natural grasping within the hand design area is a challenging task. The postures can be determined by the inter-joint rotation coordination of the fingers. Recently, Won and Robson (2019) presented a planar thumb-index finger kinematic models, applicable to the realisation of a naturalistic finger motion for robotic fingers. In the work, a naturalistic shape of fingers of the human hand is assumed as one that is observed when a human hand is grasping a (virtual) cylindroid object with an elliptical cross-section as shown in Figure 2. By maintaining numerical eccentricity (defined as e = c/a, where $c = \sqrt{(a^2 - b^2)}$) of the ellipse constant, one can obtain a joint rotation configuration kinematic model of the index finger which can be manipulated by a single control variable, either a or b. The joint angle configuration of the index finger can be obtained by formulating and solving geometric constraints which need to be met to describe the posture of the fingers when they encompass the virtual elliptic object under consideration.

Figure 2 Schematic of index finger encompassing a virtual cylindroid object (see online version for colours)

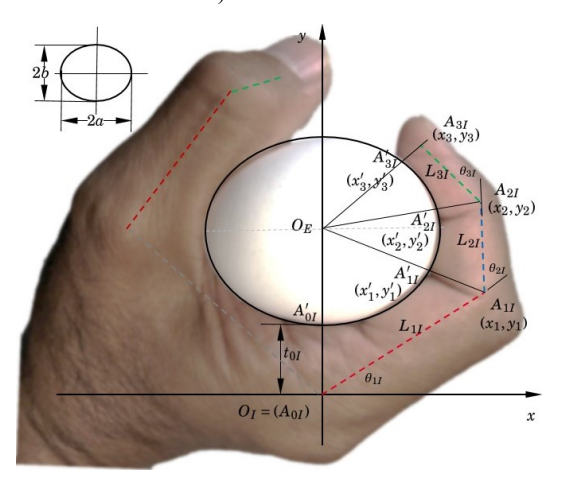


Figure 3 Joint angle calculation procedure

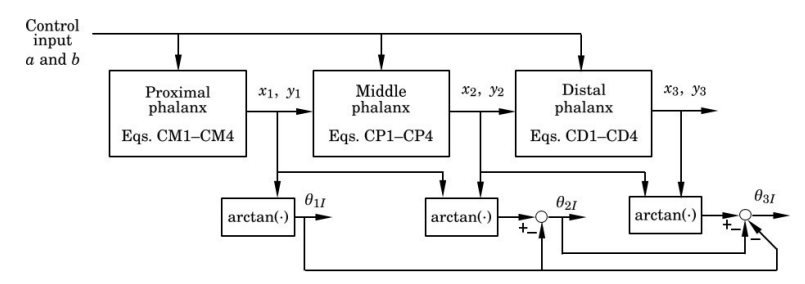
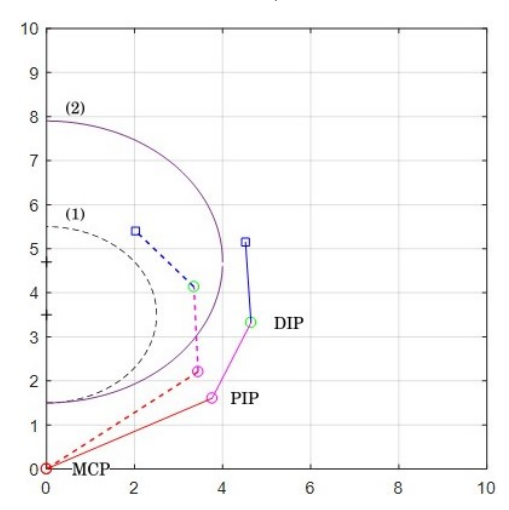
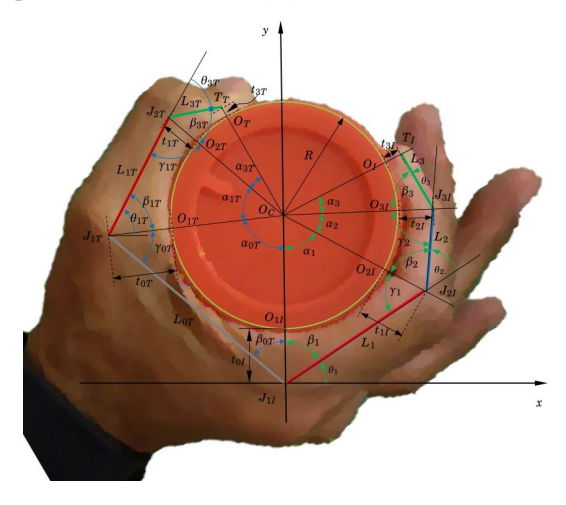


Figure 4 Example of joint rotation configuration calculation with a cylindroid of, a = 2.5 and b = 2 cm and a = 4 and b = 3.2 cm (see online version for colours)



Notes: $t_{0I}=1.5,\ t_{1I}=1.2609,\ t_{2I}=0.9321$ and $t_{3I}=0.5532$ cm, $L_{1I}=4.0895,\ L_{2I}=1.9317$ and $L_{3I}=1.8322$ cm.

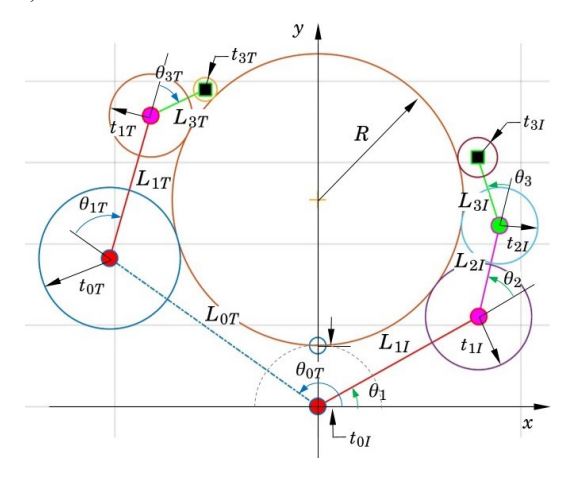
Figure 5 Schematic of index finger and thumb joint configurations encompassing a virtual cylinder (planar motion is assumed) (see online version for colours)



Notes: R is the radius of a virtual cylinder object; J_{iI} , i = 1, 2, 3 are the MCP, PIP and DIP joints, respectively; L_i is the length of phalanges of each finger; θ_i is the joint rotation angle at each joint; t_{iI} is the width from surface to skeleton (joint).

Source: Won and Robson (2019)

Figure 6 Planar problem geometry setup for a thumb and index finger system, encompassing a virtual cylinder with a radius R (planar motion is assumed) (see online version for colours)



Notes: L_i is the length of a phalanx i, t_i is the radius of joint, and θ_i is the joint rotation angle at each joint.

Figure 3 shows how the joint angle of each joint MCP, PIP, and DIP, respectively, are calculated in consecutive order. Two examples of the calculation with different sets of a and b are shown in Figure 4. Note that when a = b the object has a circular cross-section. The joint rotation configuration can be obtained numerically by solving the constraints (with a = b = R) as well as the formulas discussed in Won and Robson

(2019). In this special case, the a naturalistic shape of fingers is assumed as one that is observed when a human hand is grasping a (virtual) object with a circular cross-section.

In the model, the posture is determined by a single control parameter, i.e., the radius of a virtual circular cylinder (see Figure 5). In finding proper finger posture during grasping, the basic notion of the proposed idea is to formulate fingertip grasping as a circle configuration problem and to obtain the control parameter for the postures of fingers by solving the governing formulas. The model formularises the naturalistic finger motion during flexion or extension as closely as possible. The notion adopted to develop joint configuration models is based on the assumption that the posture of a finger which softly encompasses the surface of a virtual cylinder is similar to the one of the finger observed in the naturalistic hand defined in Figure 6. Specifically, the model has been derived based on kinematic relation on the planar thumb and index fingers and the virtual object with a circular cross-section.

Unlike inverse kinematics techniques, the resulting joint angles for the planar three degrees-of-freedom index finger are independent from each other and have the following form

$$\theta_i = \pi - \arccos(f_i(R)) - \arccos(g_i(R)), \quad i = 1, 2, 3 \tag{8}$$

where $g_1(R) = 0$ and R = R(t).

Similarly, the joint angles for the planar two degrees-of-freedom thumb are independent from each other and can be represented as:

$$\theta_{iT} = -\pi + \arccos(f_{Ti}(R)) + \arccos(g_{Ti}(R)), \quad i = 0, 1, 3$$
(9)

where $f_{T0}(R) = 0$. It is noted that the arguments of arccosine function in equations (8) and (9) have the form of a linear fractional function as $\frac{a_1R+b_1}{a_2R+b_2}$, respectively. Furthermore, note that R is the radius of a virtual circle that is used to drive joint angles of fingers and to control the degree of flexion/extension of fingers.

The Cartesian trajectory of each fingertip can be calculated using the following:

$$x_{3T} = L_{0T}\cos(\theta_{0T}) + L_{1T}\cos(\theta_{0T} + \theta_{1T}) + L_{3T}\cos(\theta_{0T} + \theta_{1T} + \theta_{3T})$$
 (10a)

$$y_{3T} = L_{0T}\sin(\theta_{0T}) + L_{1T}\sin(\theta_{0T} + \theta_{1T}) + L_{3T}\sin(\theta_{0T} + \theta_{1T} + \theta_{3T})$$
 (10b)

$$x_{3I} = L_{1I}\cos(\theta_1) + L_{2I}\cos(\theta_1 + \theta_2) + L_{3I}\cos(\theta_1 + \theta_2 + \theta_3)$$
(10c)

$$y_{3I} = L_{1I}\sin(\theta_1) + L_{2I}\sin(\theta_1 + \theta_2) + L_{3I}\sin(\theta_1 + \theta_2 + \theta_3)$$
(10d)

Determining the finger joint rotation configuration by a single control parameter R, could benefit the field of postural synergies, as well as artificial robotic hand design and controls (Moyer et al., 2013, for example). In what follows we present the idea of inter-finger coordination models, based on the notion of inter-joint coordination models described above, and experimentally evaluate them.

3 Inter-finger coordination models derived from joint coordination models and experimental evaluation

In many hand motions, several fingers work together to perform specific tasks. The notion of 'working together' can be explained in terms of the multi-finger-coordination function of the hand. The hand coordination is a combination of finger movements encompassing:

- 1 inter-joint coordination in each finger
- 2 inter-finger coordination in the hand.

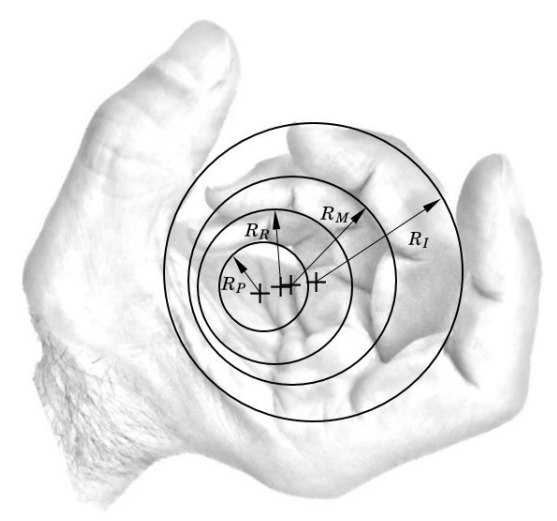
In this work, the joint configuration model outlined in Section 2 is used to expand the concept of multi-finger coordination. The notion of coordinated motions endows the model with the capability to simulate the natural characteristics of the human hand movement. As discussed in the previous section, the joint configuration model has one degree of freedom that is capable of determining each of the joint rotation angles (at the MCP, PIP and DIP joints) in the finger simultaneously by a single parameter R and representing the simplest finger movement, i.e., flexion and extension, in a simple manner. Since the model has no constraints on the angles between joints and each joint angle is independently determined by one single parameter, it can be easily used to implement inter-joint coordination.

The establishment of the profile R can be made based on the following need:

- to meet the sequence of movement in phalanges during flexion or extension movement (discussed in Carpinella et al., 2011, for example)
- 2 to form any specific shape with the fingers.

For the sequence of movement in the phalanges of a finger, the temporal aspect of inter-joint coordination has been established by imposing the time delay into R profile by providing more natural behaviour of the human finger. As mentioned earlier, the realisation of the inter-joint coordination using the proposed kinematic model is directly related to the temporal aspects of a single finger movement that considers the order of rotation initiation of each joint.

Figure 7 Example of a hand shape formed by the thumb and long fingers with different flexion degrees in fingers, which can be realised by grasping virtual cylinders with different radii each

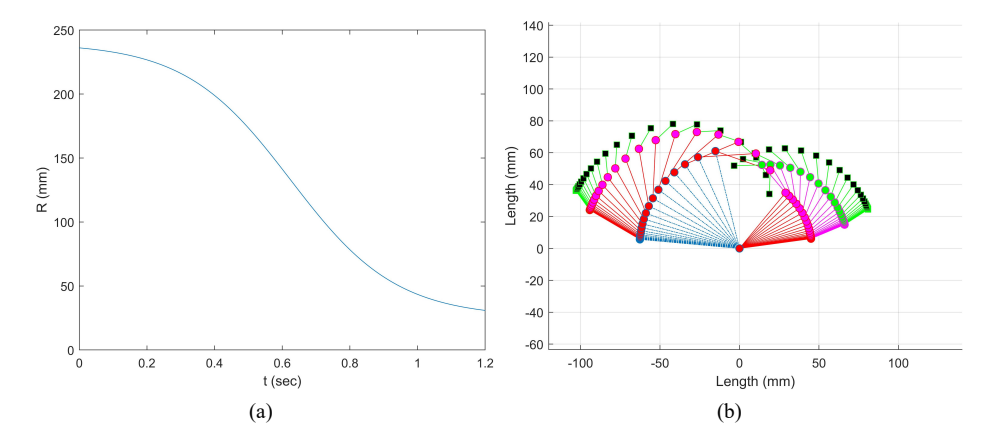


The coordination in the multi-finger level is realised in the inter-finger motion coordination block. It aims at determining human hand configurations for distinct

shapes which need to be formed by the hand for performing specific tasks, such as grasp, or object manipulation (Feix et al., 2016; Cutkosky, 1989; Yu et al., 2001, for example). The inter-finger coordination is thought to be related to the spatial aspects of multi-finger movements that consider the arrangement of virtual cylinders with different radii R_i , i = I, M, R, P, respectively, following the outputs from grasping algorithms (Bicchi, 1995; Bowers and Lumia, 2003, for example), control systems (Nagai and Yoshikawa, 1993, 1995; Nagashima et al., 1997) and a library/database of hand gesture (Molina-Vilaplana and Lopez-Coronado, 2006, for instance) to make a specific shape, as shown in Figure 7.

Let us assume that $R_I(t)$, $t \ge 0$ is given for the flexion movement of the index finger. To establish the inter-finger coordination motion discussed above, R profiles for the DIP, PIP and MCP joints can be considered as follows. Based on the above-mentioned techniques, joint rotation angles for different values of R of hyperbola function (displayed with a speed of 0.1 sec per frame) for the thumb-index fingers can be calculated. Simulation results related to the inter-joint and inter-finger coordination are shown in Figure 8.

Figure 8 Calculated joint rotation angles for changes in R of a hyperbolic function, (a) profiles of R over time, and the simulated stepwise motion of finger joints (b) thumb-index finger (displayed with a speed of 0.05 sec per frame) (see online version for colours)



In what follows we investigate how close these models define natural hand posture configuration.

3.1 Experimental evaluation of the proposed inter-finger coordination model

For the preliminary evaluation of the proposed inter-finger model, a set of motion capture experiments with a subject was performed. Optical markers were attached on the thumb, index and middle fingers of the subject, and their movement for two different grasps (power and pinch) was recorded. Specifically, for the first experiment, the subject was asked to use their thumb, index and middle fingers to perform a power grasp of a power ball, shown in Figure 9. The following semi-thickness and length (according to

Figure 5) of the thumb, index and middle fingers of the subject were considered: t_{0T} = 1.5 cm, t_{1T} = 0.8 cm, t_{3T} = 1.5 cm, L_{0T} = 5.30 cm, L_{1T} = 2.55 and L_{3T} = 1.1 cm; t_{0I} = 1.5 cm, t_{1I} = 0.9 cm, t_{2I} = 0.6 cm, t_{3I} = 0.4 cm, L_{1I} = 3.1, L_{2I} = 1.9 and L_{3I} = 1.2 cm; $t_{0M}=1.8$ cm, $t_{1M}=0.6$ cm, $t_{2M}=0.4$ cm, $t_{3M}=0.2$ cm, $L_{1M}=3.1$, $L_{2M}=1.9$ and $L_{3M} = 1.2$ cm. Through the motion capture process, the simultaneous/coordinated movement of the three fingers was recorded and the planar coordinates for joints and the fingertips, resulting from the power and precision/pinch grasping, were acquired (see Figure 9). The thumb-index-middle finger motion starting from an initial position denoted by A, going through an intermediate B, and contacting the power ball at a final position C, can be described by considering the arrangement of virtual cylinders with different radii for the three fingers to make a shape for specified time durations. At the initial location, the virtual cylinders formed by the thumb-index and thumb-middle fingers had similar time dependent profiles/radii $R_{IT} = R_{MT} = 3.05$ cm (see Table 1). At the intermediate position the thumb-index finger virtual cylinder radius becomes slightly smaller than the thumb-middle finger one ($R_{IT} = 2.60$ cm vs. $R_{MT} = 2.70$ cm) due to visual feedback of the object size and geometry, and chosen by the subject finger contact locations. At the final position, where the fingers contact the body, $R_{IT} = 2.05$ cm vs. R_{MT} = 2.45 cm. A set of joint angles was calculated for the respective time dependent parameter R using the joint angle configuration model equations, presented in Section 1. At the time of calculation, the anthropometric dimensions of each subject's fingers were considered. From the joint angles for each R, the trajectory (x, y) of the thumb, index and middle fingertips were calculated using the following:

$$x = L_1 \cos(\theta_1) + L_2 \cos(\theta_1 + \theta_2) + L_3 \cos(\theta_1 + \theta_2 + \theta_3)$$

$$y = L_1 \sin(\theta_1) + L_2 \sin(\theta_1 + \theta_2) + L_3 \sin(\theta_1 + \theta_2 + \theta_3)$$

In order to explore the extent to which the proposed model can replicate a naturalistic grasping of a stress ball motion, the joint and Cartesian fingertip trajectories from the model and the experiment were compared. The comparison of the joint angle configurations in Cartesian and joint space between the experiment and the model for the three chosen finger-object positions (initial A, intermediate B, and contact with the object C) for thumb-index-middle inter-finger coordination model for grasping of a stress ball is shown in Table 1. Joint angles of the model for each point were calculated via the equations from Section 1, with the value of R corresponding to the coordinates of the fingertip point under consideration.

During the second series of experiments, the subject was asked to grasp a small dice with their index, middle and thumb fingertips (pinch grasp), as shown in Figure 10.

For the thumb-index-middle inter-finger coordination model, a comparison of the joint angle configurations in Cartesian and joint space between the experiment and the model for three chosen locations (initial A, intermediate B and contact C) is shown in Table 2. Joint angles of the model for each point were calculated via the equations from Section 1 with the value of B corresponding to the coordinates of the fingertip point under consideration.

A general comparison between the proposed model and the preliminary experimental results in the thumb-middle-index fingers coordination for both grasping tasks shows an average joint angle difference of 3.86 degrees. This might be partially due to the fact that only the simplest circular cross-sectional shape, taken from curves of order two, was considered and tested, as well as that the current model does not take into

account the fingers-object contact conditions. Additionally, the model does not account for uncertainties associated with variations in human grasping, object geometry and/or object deformability. Overall, the preliminary results show that the finger patterns predicted by the model during the flexion/extension movement are in agreement with those obtained experimentally for both precision and power grasping. Thus, with future investigations and extensions, the proposed model could have the potential of replicating naturalistic finger motion with a high precision.

Figure 9 Experimental data collection for the power grasping task, (a) motion capture process (b) power grasp experimental data transferred and animated using Mathematica software (c) Cartesian finger trajectories (see online version for colours)

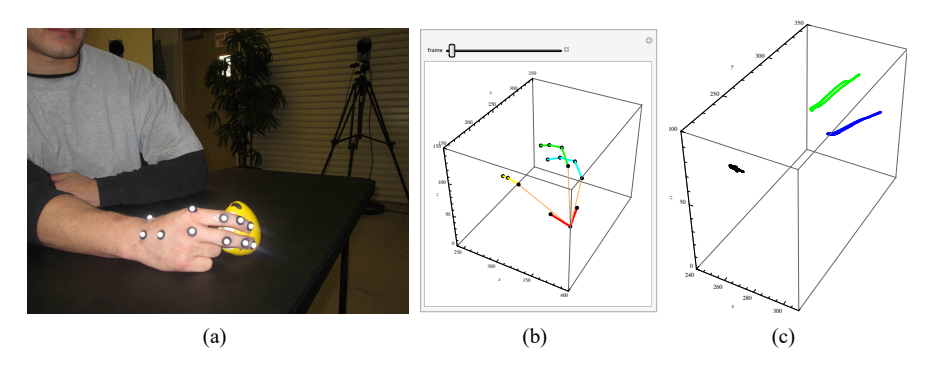
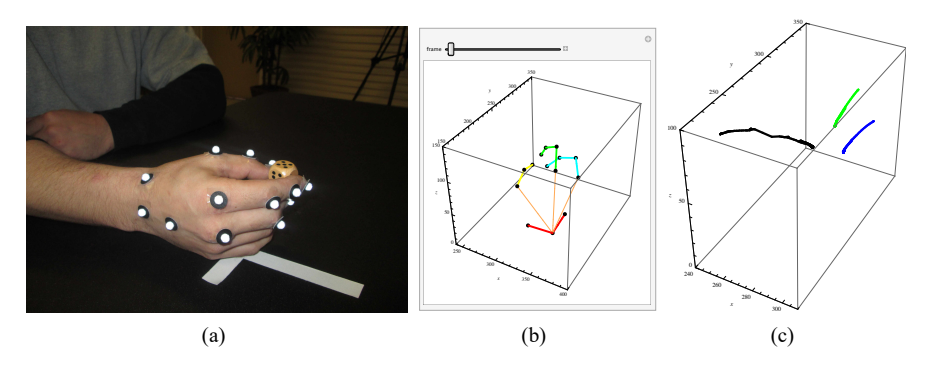


Figure 10 Experimental data collection for the precision grasping of a dice task, (a) motion capture process (b) precision grasp experimental data transferred and animated using Mathematica software (c) Cartesian finger trajectories (see online version for colours)



4 Posture determination evaluation based on predefined circle radii: case study

As a next step, evaluation of fingers' posture determination problems defined above has been performed based on the predefined values of radii and positions of the circles as listed in Table 3 (see Figure 11). The following anthropometric data of the semi-thickness and the lengths of the index finger and thumb under consideration are used for solving the equations: $t_{0I} = 15.1$, $t_{1I} = 13.1$, $t_{2I} = 9.4$ and $t_{3I} = 4.9$ mm.

 $L_1=45.4$, $L_2=22.9$ and $L_3=17.6$ mm for the index finger; $t_{0T}=17.4$, $t_{1T}=10.2$, and $t_{3T}=2.9$ mm. $L_{0T}=62.9$, $L_{1T}=36.5$ and $L_{3T}=14.9$ mm for the thumb. The correct/pre-defined value of R is 31 mm for the configuration in Figure 11. This value can be compared with the solutions from equations set for each case of different circle configurations.

Table 1 Comparison between the modelled and experimental results for three chosen fingertip trajectory locations for the proposed index-thumb-middle configuration model for grasping of a stress ball task in joint and Cartesian space

Pos. x_1, y_1 x_T, y_T x_M, y_M (cm) (cm) (cm) (cm) (cm) (deg) $(de$			x-thumb-		- R 1 T	R_{MT}				Joi	int an	gle					
mod. 3.7, 4.5 3.7, 5.9 3.2, 5.4 3.05 3.05 31 34 16 152 71 25 41 27 33 Difference (deg) 5 1 9 0 2 1 7 1 3 B Exp. 2.7, 4.8 4.0, 6.5 3.1, 5.2 2.60 2.75 34 45 24 146 69 21 38 31 40 mod. 3.0, 4.7 4.4,6.3 2.7, 5.5 2.60 2.75 34 38 28 149 69 27 43 31 35 Difference (deg) 0 7 4 3 0 6 5 0 5 C Exp. 2.0, 5.1 3.5, 6.6 1.7, 5.5 2.05 2.45 44 39 30 144 60 21 47 40 42 mod. 2.7, 4.9 3.2, 6.3 2.3, 5.5 2.05 2.45 38 36 28 146 67 30 Difference (deg) 6 3 2 2 index-thum	Pos.	x_I, y_I (cm)	x_T, y_T (cm)	x_M, y_M (cm)	(cm) (cm)	$ heta_{1I}$											
Difference (deg) B Exp. 2.7, 4.8 4.0, 6.5 3.1, 5.2 2.60 2.75 34 45 24 146 69 21 38 31 40 mod. 3.0, 4.7 4.4,6.3 2.7, 5.5 2.60 2.75 34 38 28 149 69 27 43 31 35 Difference (deg) C Exp. 2.0, 5.1 3.5, 6.6 1.7, 5.5 2.05 2.45 44 39 30 144 60 21 47 40 42 mod. 2.7, 4.9 3.2, 6.3 2.3, 5.5 2.05 2.45 38 36 28 146 67 30 Difference (deg) O 7 4 3 0 6 5 0 5 C Exp. 2.0, 5.1 3.5, 6.6 1.7, 5.5 2.05 2.45 44 39 30 144 60 21 47 40 42 mod. 2.7, 4.9 3.2, 6.3 2.3, 5.5 2.05 2.45 38 36 28 146 67 30 Difference (deg)	A Exp.	3.8, 4.2	3.8, 5.9	3.7, 4.9	3.05	3.05	26	35	25	152	69	26	34	28	36		
B Exp. 2.7, 4.8 4.0, 6.5 3.1, 5.2 2.60 2.75 34 45 24 146 69 21 38 31 40 mod. 3.0, 4.7 4.4,6.3 2.7, 5.5 2.60 2.75 34 38 28 149 69 27 43 31 35 Difference (deg) 0 7 4 3 0 6 5 0 5 C Exp. 2.0, 5.1 3.5, 6.6 1.7, 5.5 2.05 2.45 44 39 30 144 60 21 47 40 42 mod. 2.7, 4.9 3.2, 6.3 2.3, 5.5 2.05 2.45 38 36 28 146 67 30 Difference (deg) 6 3 2 2 index-thum	mod	. 3.7, 4.5	3.7, 5.9	3.2, 5.4	3.05	3.05	31	34	16	152	71	25	41	27	33		
mod. 3.0, 4.7 4.4,6.3 2.7, 5.5 2.60 2.75 34 38 28 149 69 27 43 31 35 Difference (deg) 0 7 4 3 0 6 5 0 5 C Exp. 2.0, 5.1 3.5, 6.6 1.7, 5.5 2.05 2.45 44 39 30 144 60 21 47 40 42 mod. 2.7, 4.9 3.2, 6.3 2.3, 5.5 2.05 2.45 38 36 28 146 67 30 Difference (deg) 6 3 2 2 index-thum	Differe	ence (deg	g)				5	1	9	0	2	1	7	1	3		
Difference (deg) 0 7 4 3 0 6 5 0 5 C Exp. 2.0, 5.1 3.5, 6.6 1.7, 5.5 2.05 2.45 44 39 30 144 60 21 47 40 42 mod. 2.7, 4.9 3.2, 6.3 2.3, 5.5 2.05 2.45 38 36 28 146 67 30 Difference (deg) 6 3 2 2 index-thum	B Exp.	2.7, 4.8	4.0, 6.5	3.1, 5.2	2.60	2.75	34	45	24	146	69	21	38	31	40		
C Exp. 2.0, 5.1 3.5, 6.6 1.7, 5.5 2.05 2.45 44 39 30 144 60 21 47 40 42 mod. 2.7, 4.9 3.2, 6.3 2.3, 5.5 2.05 2.45 38 36 28 146 67 30 index-thum	mod	3.0, 4.7	4.4,6.3	2.7, 5.5	2.60	2.75	34	38	28	149	69	27	43	31	35		
mod. 2.7, 4.9 3.2, 6.3 2.3, 5.5 2.05 2.45 38 36 28 146 67 30 Difference (deg) 6 3 2 2 index-thum	Differe	ence (deg	g)				0	7	4	3	0	6	5	0	5		
Difference (deg) 6 3 2 2 index-thum	C Exp.	2.0, 5.1	3.5, 6.6	1.7, 5.5	2.05	2.45	44	39	30	144	60	21	47	40	42		
100 (1) 277 277 5 177	mod	. 2.7, 4.9	3.2, 6.3	2.3, 5.5	2.05	2.45	38	36	28	146	67	30	_				
100 (1) 277 277 5 177	Difference (deg)					6	3	2	2			ind	dex-	-thur	nb.	-m	
	Average difference (deg)						3.67	3.67	5	1.67			inst	ead	l of i	nde	ΣY

Table 2 Comparison between the modelled and experimental results for three chosen fingertip trajectory locations for the proposed index-thumb configuration model for precision grasping of a dice task in joint and Cartesian space

	Index-thumb-middle			R	R_{MT}		Joint angle							
Pos.	x_I, y_I (cm)	x_T, y_T (cm)	x_M, y_M (cm)	(cm)	(cm)	$ heta_{1I}$	θ_{2I} (deg)		$ heta_{0T}$ (deg)					
A Exp.	2.6, 4.6	3.5, 6.6	2.4, 5.1	1.99	2.15	31	51	26	144	58	30	39	41	46
mod.	2.3, 5.0	2.9, 6.4	1.7, 5.5	1.99	2.15	38	47	22	143	66	33	47	41	40
Differe	nce (deg	g)				7	4	4	1	8	3	8	0	6
B Exp.	1.6, 5.0	2.3, 7.2	1.7, 5.3	1.65	2.00	41	53	25	132	53	35	44	45	43
mod.	1.5, 5.0	2.7, 6.6	1.4, 5.5	1.65	2.00	42	54	25	140	62	35	48	44	42
Differe	nce (deg	g)				1	1	0	8	9	0	4	1	1
C Exp.	0.8, 5.0	1.9, 7.2	1.4, 5.3	1.40	1.75	48	56	30	130	55	38	46	49	42
mod.	0.8, 4.9	2.1, 6.7	0.7, 5.4	1.40	1.75	45	61	28	136	64	39	52	50	45
Differe	nce (deg	g)				3	5	2	6	9	1	6	1	3
Averag	e differe	nce (deg	g)			3.67	3.33	2	5	8.67	1.33	6	0.67	3.33

4.1 Grasping an object with a circular cross-section

In this formulation, the curvature of the fingertips, object and the virtual circle (circles T, R, I, and O) are defined. With the configuration matrix **f** for TRIO configuration

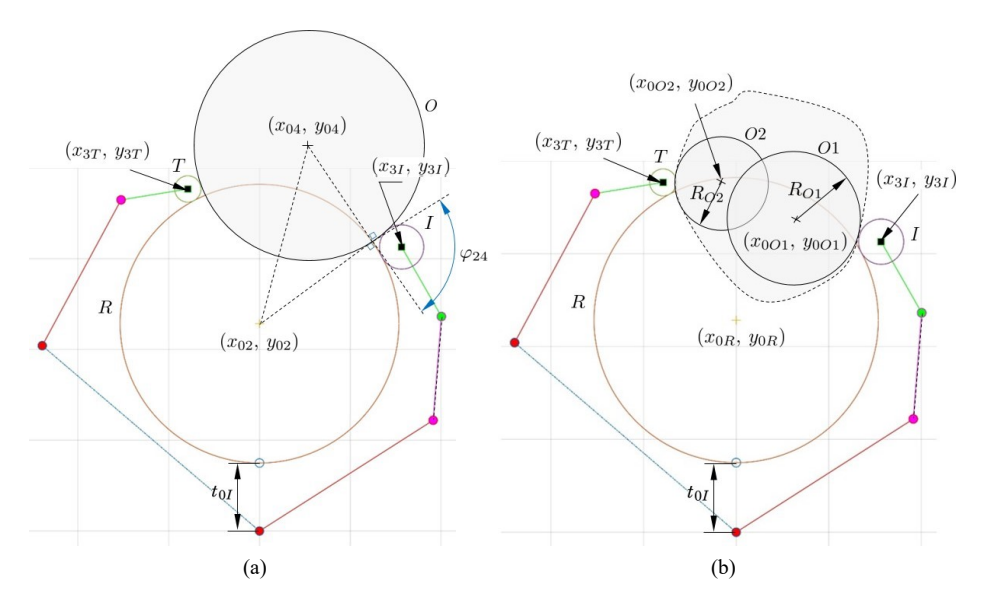
in equation (7), three equations [equations (3), (4), and (5)] are solved. As mentioned earlier, the *interaction* among circles (the fingertips and an object, precisely) can be described by defining a configuration matrix **f**. For illustrative purpose, the values of Pedoe inner product in the configuration matrix are explained first.

Table 3 Predefined radii and positions for equation solving

	Circle	Radius r_i	Centre			
	Circic	Raans 77	x_{0i}	y_{0i}		
Finger side	T	$2.9 \ (= t_{3T})$	$x_{3T} = f_{11}(R)$	$y_{3T} = f_{12}(R)$		
	R	R (unknown)	0	R + 15.1*		
	I	$4.9 \ (= t_{3I})$	$x_{3I} = f_{31}(R)$	$y_{3I} = f_{32}(R)$		
Object side	O	25.55	10.6	$(R + 15.1) + \boxed{39.8}$		
	O1	14.5	13	(R + 15.1) + 21.9		
	O2	10.2	-3.2	(R + 15.1) + 30.0		
Governing formula		Equation (3)	Equation (4)	Equation (5)		

Notes: The values in the solid-line box are information about the object being grasped and given for numerical simulation. The italic values indicate a finger model geometry setup (refer to Figure 6). A circle configuration has been made based on the priori value of R=31 mm for comparison study. (x_{3T}, y_{3T}) , thumbtip; (x_{3I}, y_{3I}) , index fingertip coordinates. (unit: mm). $*t_{0I}=15.1$.

Figure 11 Circle configuration for the case study, fingertip grasping of, (a) cylindrical object (b) object with a different curvature within the contacts (see online version for colours)



Notes: T, thumb tip circle; R, virtual circle; I, index fingertip circle; O_i , object circle(s).

The Pedoe inner product h for each configuration of two circles is given as

$$h_{13} = \frac{d_{13}^2 - r_1^2 - r_3^2}{2r_1r_3}$$

where $d_{13}^2 = (x_{01} - x_{03})^2 + (y_{01} - y_{03})^2$. $(x_{01}, y_{01}) = (x_{3T}, y_{3T})$ and $(x_{03}, y_{03}) = (x_{3I}, y_{3I})$. Note that the fingertip positions are the function of R.

2 Intersecting case: h_{24}

$$h_{24} = \cos \varphi_{24}$$

$$= \frac{d_{24}^2 - r_2^2 - r_4^2}{2r_2r_4}$$

where φ_{24} is the angle of intersection between c_2 and c_4 . This can be used as a degree of grasping. $d_{24}^2 = (x_{04} - x_{02})^2 + (y_{04} - y_{02})^2$ and $(x_{02}, y_{02}) = (0, R + t_{0I})$. $r_2 = R$. (x_{04}, y_{04}) , the centre of object, is assumed to be given priorly.

Tangent (external/internal) case: Not explicitly listed in the entries in f_{TRIO} , if two circles are tangent each other, then $h_{ij} = 1$.

$$h_{12} = h_{21} = 1, h_{14} = h_{41} = 1, h_{23} = h_{32} = 1, h_{34} = h_{43} = 1$$

When a soft finger grasping is considered (i.e. the finger tip experiences small deformation when grasping an object) the interaction between the circles can be seen as an intersecting case. Both $h_{14} = h_{41}$ and $h_{34} = h_{43}$ can be calculated by the following:

$$h_{14} = \cos \varphi_{14}$$

$$= \frac{d_{14}^2 - r_1^2 - r_4^2}{2r_1r_4}$$

where $d_{14}^2 = (x_{01} - x_{04})^2 + (y_{01} - y_{04})^2$. Note again that $x_{01} = f_{11}(R)$ and $y_{01} = f_{12}(R)$.

$$h_{34} = \cos \varphi_{34}$$

$$= \frac{d_{34}^2 - r_3^2 - r_4^2}{2r_3r_4}$$

where $d_{34}^2 = (x_{03} - x_{04})^2 + (y_{03} - y_{04})^2$. Note again that $x_{03} = f_{31}(R)$ and $y_{03} = f_{32}(R)$.

It is thought that quantifying the amount of small deformation during grasping as the angle of intersection between fingertips and object is one way to deal with soft finger grasping issue. An interaction relation between hand and object can be obtained by applying the configuration matrix defined above to equations (3), (4) and (5). Equation (3) yields a relation among curvatures of circles and equations (4) and (5) yield relations among curvatures and positions of circles.

The fingertip positions shown in equation (10) are functions of the control parameter R and they are complicated mainly due to the trigonometric characteristics of joint rotation angles. This leads to challenges in the expansion and manipulation of $\mathbf{F} = \mathbf{f}^{-1}$.

To lessen computational strains considerably, they are replaced with an approximated version of functions, obtained by curve fitting. The following is a set of approximated version with an anthropometric data from the hand of the specific subject, given in the beginning of the section. The range of R is set to be [25 mm, 240 mm].

$$x_{3T} = f_{11}(R) = 2.2 \cdot 10^{-7} R^4 - 0.00014 R^3 + 0.035 R^2 - 3.9 R + 73$$
 (11a)

$$y_{3T} = f_{12}(R) = -1.3 \cdot 10^{-7} R^4 + 7.3 \cdot 10^{-5} R^3 - 0.014 R^2 + 0.69 R + 66$$
 (11b)

$$x_{3I} = f_{31}(R) = 1.4 \cdot 10^{-9} R^5 - 1.1 \cdot 10^{-6} R^4 - 0.00032 R^3 - 0.049 R^2 + 3.8 R - 46$$

$$-0.049R^{2} + 3.8R - 46$$

$$y_{3I} = f_{32}(R) = -3.5 \cdot 10^{-6}R^{3} + 0.0024R^{2} - 0.6R + 79$$
(11d)

For the configuration setting, the equations are solved and the results are given in Table 4. It is thought that the slightly different values could possibly be due to the fact that the coordinate of the fingertip was expressed using an approximation formula and/or due to calculation error that occurs when the solution of the nonlinear higher-order equation is sought. It is worth noting that when the hand fully encompasses a circular object (i.e., $C_3 = C_4$), the configuration matrix ${\bf f}$ for the circle configuration is constructed as

$$\mathbf{f}_{\text{TRIO}} = \begin{bmatrix} -1 & 1 & h_{13} & 1\\ 1 & -1 & 1 & -1\\ h_{13} & 1 & -1 & 1\\ -1 & -1 & 1 & -1 \end{bmatrix}$$
(12)

This circle configuration does not guarantee independence of circles. The rank of matrix **f** is three, **F** can not be found, as expected. Thus, it is not possible to get an interaction relation between the fingertips and an object to be grasped for this case.

Table 4 Simulation results for TRIO configuration

	Circle	Radius r_i	Centre				
	Circic	Raarus 17	x_{0i}	y_{0i}			
Finger side (joint angle model)	C_1 (T)	2.9	$x_{3T} = f_{11}(R)$	$y_{3T} = f_{12}(R)$			
	C_2 (R)	R (unknown)	0	R + 15.1			
	C_3 (I)	4.9	$x_{3I} = f_{31}(R)$	$y_{3I} = f_{32}(R)$			
Object side	C_4 (O)	25.55	10.6	(R + 15.1) + 39.8			
Interaction relation		Equation (3)	Equation (4)	Equation (5)			
Solution R		14.58	14.56	14.12			
		29.34	30.20	29.79			

Notes: The values in the solid-line box are information about the object being grasped and given for numerical simulation. The italic values indicate a finger model setup. A circle configuration has been made based on the priori value of R=31 mm for comparison study. (x_{3T}, y_{3T}) , thumbtip; (x_{3I}, y_{3I}) , index fingertip coordinates (unit: mm).

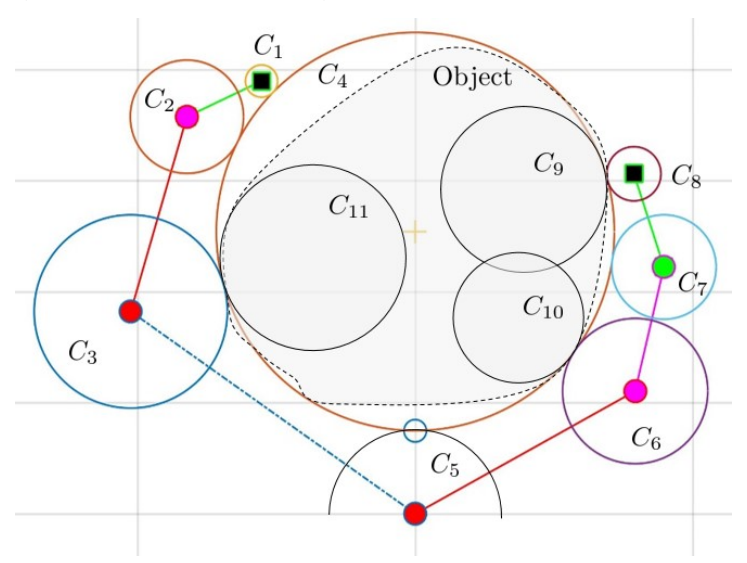
4.2 Grasping an object with different curvature within the contact

For the case shown in Figure 1(b), five possible circle configurations can be defined. For each configuration, equations are constructed and solved to obtain the control parameter R which guarantees fingertip grasping under consideration. Table 5 lists the solutions from the equations solving for different cases of circle configuration. The correct/a priori given value of R can be set if appropriate conditions are imposed. As mentioned before, the value of R was set to be 31 mm. It is noted that because of the difference in the degree of polynomial from curve fitting in equation (11) and in the combination of circles, the number of solutions is different.

Table 5	Results	of eq	uations	solving	tor	different	cases

Circle		R from	_
configuration	Equation (3)	Equation (4)	Equation (5)
TIO1O2	4.22, 14.31, 30.13, 30.45,	13.03, 30.09	13.07, 30.07, 30.96, 153.96
	74.95		
TRO1O2	16.41, 29.64	21.11, 38.94	16.90, 29.86
RIO1O2	6.53, 13.16, 15.52, 30.25	12.51, 13.73, 21.35, 30.48	16.46, 30.40
TRIO1	13.30, 30.11	12.47, 39.83	10.92, 30.51
TRIO2	16.71, 29.51	19.89, 30.31	16.96, 30.09

Figure 12 Selection of four circles for solving problem of grasping a specific type of object (see online version for colours)



As shown in Figure 12, depending on the characteristics of the object being grasped, the control/posture configuration parameter R can be calculated by taking any four circles from the fingers-object geometry setup.

5 Conclusions

In this paper, a recently developed planar finger kinematic model for natural motion is experimentally evaluated. Overall, the preliminary results show that the finger patterns predicted by the model during the flexion/extension movement are in agreement with those obtained experimentally for both precision and power grasping. Thus, with future investigations and extensions, the proposed model could have the potential of replicating naturalistic finger motion with a high precision. As a next step, it is studied if the model could be combined with circle configuration techniques based on Pedoe maps to explore the relation between the fingertips-object contact curvature and the posture configuration for precision grasping applications. Within the proposed planar contact geometry setup the fingertips and object curvatures in the vicinity of the contacts are represented by circles with different radii. The results show that it is possible to calculate the posture configuration based on the choice of any four circles. Moreover, when grasping an object with a circular cross-section, the configuration matrix does not guarantee independence of circles and thus, it is not possible to get an interaction relation between the fingertips and the object. In cases where the configuration parameter is defined, there are four different scenarios and if the posture configuration parameter is not known, both the object geometry within the contacts and the curvature of each fingertip could be specified. Future directions include exploring ways to incorporate fingertip curvature and/or posture along with the object curvature within the kinematic synthesis of grasping and manipulation tasks in order to enable novel future combined design-control strategies.

Acknowledgements

The authors gratefully acknowledge the support of NSF CAREER award ID 1751770.

References

- Barbagli, F., Frisoli, A., Salisbury, K. and Bergamasco, M. (2004) 'Simulating human fingers: a soft finger proxy model and algorithm', in *HAPTICS'04 Proceedings, 12th International Symposium on Haptic Interfaces for Virtual Environment and Teleoperator Systems*, Chicago, IL, 27–28 March, pp.9–17.
- Bicchi, A., Gabiccini, M. and Santello, M. (2011) 'Modeling natural and artificial hands with synergies', in *Philosophical Transactions*, Vol. 366, No. 1581, pp.3153–3161.
- Bicchi, A. (1995) 'On the closure properties of robotic grasping', *The International Journal of Robotics Research*, Vol. 14, No. 4, pp.319–334.
- Bowers, D. and Lumia, R. (2003) 'Manipulation of unmodeled objects using intelligent grasping schemes', *IEEE Transactions on Fuzzy Systems*, Vol. 11, No. 3, pp.320–330.
- Braido, P. and Zhang, X. (2004) 'Quantitative analysis of finger motion coordination in hand manipulative and gestic acts', *Hum. Mov. Sci.*, Vol. 22, No. 6, pp.661–678.
- Carpinella, I., Jonsdottir, J. and Ferrarin, M. (2011) 'Multi-finger coordination in healthy subjects and stroke patients: a mathematical modeling approach', *J. NeuroEng. Rehabil.*, Vol. 8, No. 19, pp.1–19.
- Cutkosky, M. (1989) 'On grasp choice, grasp models and the design of hands for manufacturing tasks', *IEEE Transactions on Robotics and Automation*, Vol. 5, No. 3, pp.269–279.

- Darboux, G. (1872) 'Sur les relations entre les groupes de points, de cercles et de sphères dans le plan et dans lèespace', *Ann. Sci. Ècole Norm*, Vol. 1, pp.323–392 [online] http://www.numdam.org/article/ASENS\ 1872 2 1 323 0.pdf.
- Descartes, R. (1901) 'Oeuvres de Descartes', in Adam, C. and Tannery, P. (Eds.): *Correspondence IV*, Leopold Cerf., Paris.
- Feix, T., Romero, J., Schmiedmayer, H., Dollar, A.M. and Kragic, D. (2016) 'The GRASP taxonomy of human grasp types', *IEEE Transactions on Human-Machine Systems*, Vol. 46, No. 1, pp.66–77.
- Kim, B.H. (2014) 'Analysis of coordinated motions of humanoid robot fingers using inter-phalangeal joint coordination', *Int. J. Adv. Rob. Syst.*, Vol. 11, No. 69, pp.1–8.
- Kocik, J. (2007) A Theorem on Circle Configurations, Mathematics Department, CIU, Apollonian Seminar.
- McDonald, J., Toro, J., Alkoby, K., Berthiaume, A., Carter, R., Chomwong, P., Christopher, J., Davidson, M.J., Furst, J., Konie, B., Lancaster, G., Roychoudhuri, L., Sedgwick, E., Tomuro, N. and Wolfe, R. (2001) 'An improved articulated model of the human hand', *Vis. Comput.*, Vol. 17, No. 8, pp.158–166.
- Miyata, N., Kouchi, M., Mochimaru, M., Kawachi, L. and Kurihara, T. (2005) 'Hand link modeling and motion generation from motion capture data based on 3D joint kinematics', in SAE 2005 Digital Human Modeling for Design and Engineering Symposium, Iowa City, IA, 14–16 June, No. 2005-01-2687.
- Miyata, N., Kouchi, M. and Mochimaru, M. (2007) 'Generation and validation of 3D links for representative hand models', in SAE 2007 Digital Human Modeling for Design and Engineering Conference, Seattle, WA, 12–14 June, No. 2007-01-2512.
- Molina-Vilaplana, J. and Lopez-Coronado, J. (2006) 'A neural network model for coordination of hand gesture during reach to grasp', *Neural Network*, Vol. 19, pp.12–30, DOI: 10.1016/j.neunet.2005.07.014.
- Moyer, T., Faulrig, E.L. and Santos-Munne, J.J. (2013) One Motor Finger Mechanism, U.S. Patent No. 8470051B2.
- Nagai, K. and Yoshikawa, T. (1993) 'Dynamic manipulation/grasping control of multifingered robot hands', in *Proceedings of IEEE International Conference on Robotics and Automation*, Atlanta, GA, 2–6 May, pp.1027–1033.
- Nagai, K. and Yoshikawa, T. (1995) 'Grasping and manipulation by arm/multifingered-hand mechanisms', in *Proceedings of IEEE International Conference on Robotics and Automation*, Nagoya, Japan, 21–27 May, pp.1040–1047.
- Nagashima, T., Seki, H. and Tanako, M. (1997) 'Analysis and simulation of grasping/manipulation by multi-finger surface', Mechanism and Machine Theory, Vol. 32, No. 2, pp.175–191.
- Nolker, C. and Ritter, H. (2002) 'Visual recognition of continuous hand postures', in *IEEE Trans. Neural Netw.*, Vol. 13, No. 4, pp.983–994.
- Pedoe, D. (1957) On Circles, A Mathematical View, Dover, 1979, Dover Publications, New York.
- Pedoe, D. (1967) 'On a theorem in geometry', *Amer. Math. Monthly*, Vol. 74, pp.627–640, DOI: 10.1080/00029890.1967.12000012.
- Pedoe, D. (1970) Geometry, A Comprehensive Course, Dover, 1980, Dover Publications, New York.
- Pena-Pitarch, E., Falguera, N.T. and Yang, J.J. (2012) 'Virtual human hand: model and kinematics', in *Comput. Methods Biomech. Biomed. Eng.*, Vol. 17, No. 5, pp.568–579.
- Rimon, E. and Burdick, J.W. (1995a) 'A configuration space analysis of bodies in contact I. 1st order mobility', *Mechanism and Machine Theory*, Vol. 30, No. 6, pp.897–912.
- Rimon, E. and Burdick, J.W. (1995b) 'A configuration space analysis of bodies in contact II. 2nd order mobility', *Mechanism and Machine Theory*, Vol. 30, No. 6, pp.913–928.

- Robson, N. and Chen, B. (2019) 'Geometric design with multiple realizable motion tasks in the vicinity of a planar mechanism-environment contact', *Journal of Mechanisms and Robotics*, Vol. 11, No. 4, 041007-4.
- Robson, N.P. and McCarthy, J.M. (2007) 'Kinematic synthesis with contact direction and curvature constraints on the workpiece', in *Proceedings of ASME International Design Engineering Technical Conferences and Computers and Information in Engineering Conference*, Las Vegas, Nevada
- Robson, N.P. and McCarthy, J.M. (2009) 'Applications of the geometric design of mechanical linkages with task acceleration specifications', in ASME International Design Engineering Technical Conferences and Computers and Information in Engineering Conference, San Diego, California.
- Robson, N.P. and McCarthy, J.M. (2010) 'Second order task specifications in the geometric design of spatial mechanical linkages', *International Journal of Modern Engineering*, Vol. 11, pp.5–11.
- Robson, N. and Soh, G.S. (2018) 'Kinematic synthesis of planar multi-limb mechanisms for multi-directional interaction with objects in the environment', in *International Symposium on Advances in Robot Kinematics*, Springer, pp.356–363.
- Robson, N. and Tolety, A. (2011) 'Geometric design of spherical serial chains with curvature constraints in the environment', in *ASME International Design Engineering Technical Conferences and Computers and Information in Engineering Conference*, Washington, DC.
- Robson, N., Ghosh, S. and McCarthy, J.M. (2015) 'Simultaneous geometric design of mechanical fingers for coordinated movement', in 14th IFToMM World Congress, Taipei, Taiwan.
- Santello, M., Flanders, M. and Soechting, J.F. (1998) 'Postural synergies for tool use', *The Journal of Neuroscience: The Official Journal of the Society for Neuroscience*, December, Vol. 17, No. 23, pp.10105–10115, DOI: 10.1523/JNEUROSCI.18-23-10105.1998.
- Savescu, A., Cheze, L., Wang, X., Beurier, G. and Verriest, J. (2004) 'A 25 degrees of freedom hand geometrical model for better hand attitude simulation', in *SAE 2004 Digital Human Modeling for Design and Engineering Symposium*, Rochester, MI, 15–17 June, No. 2004-01-2196.
- Won, J.S. and Robson, N. (2019) 'Control-oriented human finger kinematic model: geometry based approach', Journal of Mechanisms and Robotics, DOI: 10.1115/1.4044601.
- Yu, Y., Li, Y. and Tsujio, S. (2001) 'Analysis of finger position regions on grasped object with multifingered hand', in *Proceedings of the 2001 IEEE International Symposium on Assembly and Task Planning (ISATP2001)*, Fukuoka, Japan, 28–30 May, pp.178–183.